JACS
JOURNAL OF THE AMERICAN CHEMICAL SOCIETY

Article

Comparative Gas Sensing in Cobalt, Nickel, Copper, Zinc, and Metal-Free Phthalocyanine Chemiresistors

Forest I. Bohrer, Corneliu N. Colesniuc, Jeongwon Park, Manuel E. Ruidiaz, Ivan K. Schuller, Andrew C. Kummel, and William C. Trogler

J. Am. Chem. Soc., **2009**, 131 (2), 478-485• DOI: 10.1021/ja803531r • Publication Date (Web): 18 December 2008

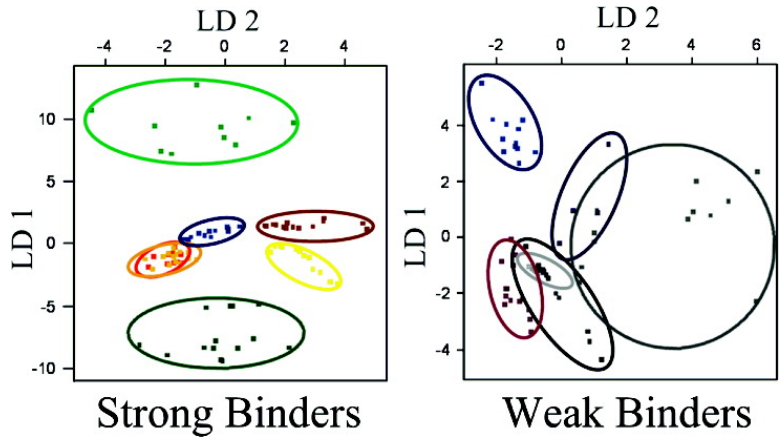

More About This Article

Additional resources and features associated with this article are available within the HTML version:

- Supporting Information
- Access to high resolution figures
- Links to articles and content related to this article
- Copyright permission to reproduce figures and/or text from this article

View the Full Text HTML

Journal of the American Chemical Society is published by the American Chemical Society. 1155 Sixteenth Street N.W., Washington, DC 20036

J|A|C|S ARTICLES

Published on Web 12/18/2008

Comparative Gas Sensing in Cobalt, Nickel, Copper, Zinc, and Metal-Free Phthalocyanine Chemiresistors

Forest I. Bohrer,[†] Corneliu N. Colesniuc,[§] Jeongwon Park,[‡] Manuel E. Ruidiaz,[⊥] Ivan K. Schuller,*[,§] Andrew C. Kummel,*[,†] and William C. Trogler*[,†]

Department of Chemistry and Biochemistry, Materials Science and Engineering Program, Department of Physics, and Department of Bioengineering, University of California, San Diego, 9500 Gilman Drive, La Jolla, California 92093

Received May 12, 2008; E-mail: ischuller@ucsd.edu; akummel@ucsd.edu; wtrogler@ucsd.edu

Abstract: The sensitivities of metallophthalocyanine (MPcs: M = Co, Ni, Cu, Zn, and H_2) chemiresistors to vapor phase electron donors were examined using 50 nm MPc films deposited on interdigitated electrodes. Sensor responses were measured as changes in current at constant voltage. Analytes were chosen to span a broad range of Lewis base and hydrogen bond base strengths. The MPc sensor responses were correlated exponentially with binding enthalpy. These exponential fits were consistent with the van't Hoff equation and standard free energy relationships. Sensor recovery times were found to depend exponentially on binding enthalpy, in agreement with the Arrhenius equation. Relative sensitivities of all MPcs were compared via two-way ANOVA analysis. Array response patterns were differentiated via linear discriminant analysis, and analyte identification was achieved over a range of concentrations with 95.1% classification accuracy for the strong binding analytes. The ability to distinguish among different analytes, regardless of their concentration, through normalization of the responses to a reference sensor is particularly noteworthy.

1. Introduction

Phthalocyanines (Pcs), both metalated (MPcs) and metal-free (H_2Pc), are metal−organic semiconductors that have been applied as chemiresistive sensors.[1−3] MPc sensitivity to vapor-phase molecules may be tuned by manipulation of the metal center and by substitution of functional groups on the organic ring.[1−4] Conductivity in MPc films depends strongly on atmospheric chemical species, particularly oxidants and reductants.[5,6] P-type MPcs are insulating in dark, high-vacuum environments and become semiconducting on exposure to air.[7−9] This air-induced conductivity has been attributed to coordination of O_2 to surface MPc metal centers, forming superoxide adducts which extract electrons, generating charge carriers (holes) in the bulk film.[10−12] Superoxide adducts have been detected directly through EPR studies.[13−15] Oxygen adsorption on H_2Pc has been reported as occurring on the four *meso*-nitrogens, leading to weaker conductivity gains.[16] Other oxidizing gases (O_3, NO_X, Cl_2, and others) induce similar conductivity gains in p-type MPc films through charge transfer or redox reactions which generate holes in the film.[17−20] Similar charge transfer interactions have been used to identify nitrated explosives in conjunction with pattern recognition algorithms.[21]

MPc interactions with electron-donating (reducing) gases, including Lewis bases such as NH_3, have the opposite effect. Current losses reported on dosing with Lewis bases have been attributed to hole trapping within the p-type film by electrons donated from the chemisorbed analyte.[5] Sensor interactions with electron donating analytes may be understood by using linear solvation energy relationships (LSER), which account for weak

[†] Department of Chemistry and Biochemistry.
[‡] Materials Science and Engineering Program.
[§] Department of Physics.
[⊥] Department of Bioengineering.

(1) Snow, A. W.; Barger, W. R. Phthalocyanine Films in Chemical Sensors. In *Phthalocyanines: Properties and Applications*; Lever, A. B. P., Ed; John Wiley and Sons: New York, 1989; Vol. 1, p 341.
(2) Eley, D. *Nature* **1948**, *162*, 819.
(3) Gould, R. D. *Coord. Chem. Rev.* **1996**, *156*, 237–274.
(4) Guillaud, G.; Simon, J.; Germain, J. *Coord. Chem. Rev.* **1998**, *178*, 1433–1484.
(5) Schollhorn, B.; Germain, J. P.; Pauly, A.; Maleysson, C.; Blanc, J. P. *Thin Solid Films* **1998**, *326*, 245–250.
(6) Germain, J. P.; Pauly, A.; Maleysson, C.; Blanc, J. P.; Schollhorn, B. *Thin Solid Films* **1998**, *333*, 235–239.
(7) Martin, M.; Andre, J. J.; Simon, J. *J. Appl. Phys.* **1983**, *54*, 2792–2794.
(8) Pankow, J. W.; Arbour, C.; Dodelet, J. P.; Collins, G. E.; Armstrong, N. R. *J. Phys. Chem.* **1993**, *97*, 8485–8494.
(9) Hiller, S.; Schlettwein, D.; Armstrong, N. R.; Wohrle, D. *J. Mater. Chem.* **1998**, *8*, 945–954.
(10) Kerp, H. R.; Westerduin, K. T.; van Veen, A. T.; van Faassen, E. E. *J. Mater. Res.* **2001**, *16*, 503–511.
(11) Simon, J.; Andre, J. J. *Molecular Semiconductors*; Springer-Verlag: Berlin, 1985; pp 73−149.
(12) Ho, K. C.; Tsou, Y. H. *Sens. Actuators, B* **2001**, *77*, 253–259.
(13) Zwart, J.; Van Wolput, J. H. M. C. *J. Mol. Catal.* **1979**, *5*, 51–64.
(14) Yahiro, H.; Naka, T.; Kuramoto, J.; Kurohagi, K.; Okada, G.; Shiotani, M. *Microporous Mesoporous Mater.* **2005**, *79*, 291–297.
(15) Barbon, A.; Brustolon, M.; van Faassen, E. E. *Phys. Chem. Chem. Phys.* **2001**, *3*, 5342–5347.
(16) Wright, J. D. *Prog. Surf. Sci.* **1989**, *31*, 1–60.
(17) Lee, Y. L.; Tsai, W. C.; Chang, C. H.; Yang, Y. M. *Appl. Surf. Sci.* **2001**, *172*, 191–199.
(18) Sadaoka, Y.; Jones, T. A.; Gopel, W. *Sens. Actuators, B* **1990**, 148–153.
(19) Miyata, T.; Minami, T. *Appl. Surf. Sci.* **2005**, *244*, 563–567.
(20) Sadaoka, Y.; Jones, T. A.; Gopel, W. *J. Mater. Sci. Lett.* **1989**, *8*, 1288–1290.
(21) Ponnu, A.; Edwards, N. Y.; Anslyn, E. V. *New J. Chem.* **2008**, *32*, 848–855.

10.1021/ja803531r CCC: $40.75

Scheme 1. Model of Chemisorption onto MPc Film by Coordinating Analyte L; Analytes May Bind at Open Metal Sites or May Compete for Oxygen-Bound Sites

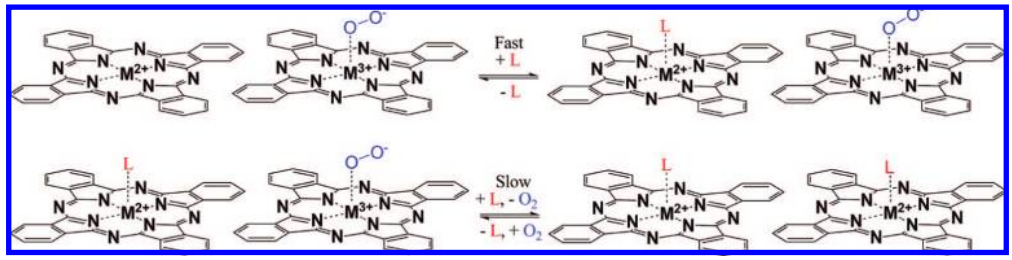

intermolecular forces such as dispersion interactions (van der Waals forces and $\pi-\pi$ interactions), polarizability, dipolarity, and hydrogen bond acidity and basicity.[22,23] Though not included in general LSER theory, metal coordinative bonds are potentially the strongest intermolecular binding force for adsorption of Lewis bases onto MPcs.[24] As a surface dopant, O_2 occupies only a fraction of the binding sites on the film;[10] therefore, strong electron donors can bind either to oxygen-free surface metal centers or compete with O_2 for occupied metal surface sites (Scheme 1).[25] For weak electron donors, it is possible to have physisorption to the organic phthalocyanine ring through van der Waals forces and polarization interactions. These weak interactions are consistent with the weak sensor responses seen for these analytes.

Detection of electron-donating analytes by CoPc was found to be governed primarily by coordination to the metal center.[25] CoPc sensor responses to these analytes were correlated bilinearly to the Lewis basicity of the analyte, described by the binding enthalpy scale $-\Delta H^{\circ}_{BF_3}$.[26] The $-\Delta H^{\circ}_{BF_3}$ scale was determined from calorimetrically measured enthalpies of formation (kJ mol−1) of 1:1 adducts of Lewis bases to the Lewis acid BF_3 in dichloromethane, thereby directly probing basicity through the free energy of binding. Detection of electron donors by H_2Pc was bilinearly correlated with the hydrogen bond basicities of the analytes as tabulated in the β_2^H scale.[25,27] Values for the β_2^H scale were determined using log K values (dm^3 mol^{-1}) of the complexation of bases with reference acids such as 4-fluorophenol in CCl_4. Therefore, the β_2^H scale is an indirect probe of basicity and binding enthalpy through reaction equilibria.

Arrays of MPc sensors (VOPc, TiOPc, CoPc, NiPc, CuPc, ZnPc, and PbPc) have been used to detect various analytes, including strongly basic analytes such as pyridine and piperidine,[28,29] hydrocarbons and aromatic compounds (hexane, benzene, and toluene),[29,30] polar[31] and protic[32] solvents (acetonitrile, THF, methanol, and isopropanol), and strong oxidants such as NO and NO_2.[33] However, none of these studies examines a spectrum of analytes with a broad range of binding strengths. In the present study the sensitivities of an array of MPc chemiresistors (M = Co, Ni, Cu, Zn, and H_2) are examined with respect to a series of analytes spanning a range of both Lewis basicities ($-\Delta H^{\circ}_{BF_3}$) and hydrogen bond basicities (β_2^H). Sensor kinetics are examined to determine the dependence of sensor recovery on analyte basicity. The MPc device sensitivities are compared via two-way ANOVA analysis. Linear discriminant analysis is employed for analyte identification for a range of concentrations, and normalization is shown to provide a concentration-independent method for analyte identification.

2. Experimental Section

2.1. Sensor Fabrication. Chemiresistive metallophthalocyanine (MPc) sensors were prepared as reported previously.[25] 50 nm thick Au interdigitated electrodes (IDEs) were prepared by standard photolithography and processing on 1 μm-thick SiO_2 over (100) Si substrates; the IDEs contained 45 finger pairs with a channel length of 5 μm and a width of 2 mm. Six IDEs were fabricated per substrate for reproducibility and chip fabrication used the clean room facilities at the California Institute for Telecommunications and Information Technology (Calit2) at UCSD. CoPc (Aldrich, 97%), NiPc (Aldrich, 85%), CuPc (Aldrich, 97%), ZnPc (Acros, 98%), and H_2Pc (Aldrich, 98%) were purified by multiple zone sublimations at 400 °C and 10^{-5} Torr. The 50 nm thick sensor films of MPcs were deposited on IDEs in a UHV chamber (base pressure 2×10^{-10} Torr) using organic molecular beam epitaxy (deposition pressure 5×10^{-9} Torr, deposition rate 0.2 − 0.5 Å s^{-1}). Deposition rate and film thickness were monitored by QCM. Substrate temperature during deposition was held constant at 25.0 ± 0.1 °C to maintain constant film morphology across all sensors. Film thickness and structure were characterized by low angle XRD measurements (Rigaku RU-200B diffractometer, Cu Kα radiation) and AFM (Nanoscope IV Scanning Microscope, Mikromasch NSC15 325 kHz probe, Figure 1).[34] The devices were aged at 10 mTorr for 48 h before use.

2.2. Device Measurements. Sensor responses of MPc chemiresistors were measured as reported previously.[25] Each array of six IDEs was wirebonded to leads in a dual in-line ceramic package purchased from Spectrum Semiconductor Materials, Inc. (Figure 1). Two sensor arrays were mounted simultaneously in a SiO_2-passivated stainless steel chamber (15 cm^3 internal volume). Sensors were monitored by a Keithley 6517/6521 multichannel electrometer used as both the voltage source and ammeter. Any residual sensor photoconductivity was allowed to decay for 24 h before testing.

(22) Grate, J. W.; Abraham, M. H. *Sens. Actuators, B* **1991**, *3*, 85–111.
(23) Grate, J. W. *Chem. Rev.* **2000**, *100*, 2627–2648.
(24) Liao, M. S.; Kar, T.; Gorun, S. M.; Scheiner, S. *Inorg. Chem.* **2004**, *43*, 7151–7161.
(25) (a) Bohrer, F. I.; Sharoni, A.; Colesniuc, C.; Park, J.; Schuller, I. K.; Kummel, A. C.; Trogler, W. C. *J. Am. Chem. Soc.* **2007**, *129*, 5640–5646. (b) Park, J.; Yang, R. D.; Colesniuc, C.; Sharoni, A.; Jin, S.; Schuller, I. K.; Trogler, W. C.; Kummel, A. C. *Appl. Phys. Lett.* **2008**, *92*, 193311.
(26) Maria, P. C.; Gal, J. F. *J. Phys. Chem.* **1985**, *89*, 1296–1304.
(27) Abraham, M. H.; Grellier, P. L.; Prior, D. V.; Morris, J. J.; Taylor, P. J. *J. Chem. Soc., Perkins Trans 2* **1990**, 521–529.
(28) Spadavecchia, J.; Ciccarella, G.; Rella, R. *Sens. Actuators, B* **2005**, *106*, 212–220.
(29) Sibrina, G. V.; Blokhina, S. V.; Ol'kovich, M. V.; Borovkov, N. Yu. *Russ. J. Gen. Chem.* **1997**, *67* (3), 479–484.
(30) Sibrina, G. V.; Blokhina, S. V.; Ol'kovich, M. V.; Borovkov, N. Yu. *Russ. J. Gen. Chem.* **1997**, *67* (3), 439–444.
(31) Bora, M.; Schut, D.; Baldo, M. A. *Anal. Chem.* **2007**, *79*, 3298–3303.
(32) Yang, R. D.; Fruhberger, B.; Park, J.; Kummel, A. C. *Appl. Phys. Lett.* **2006**, *88*, 074104/1–074104/3.
(33) Chen, J. C.; Ju, Y. H.; Liu, C. J. *Sens. Actuators, B* **1999**, *60*, 168–173.
(34) (a) Miller, C. W.; Sharoni, A.; Liu, G.; Colesniuc, C. N.; Fruhberger, B.; Schuller, I. K. *Phys. Rev. B* **2005**, *72*, 104113/1–104113/6. (b) Liu, G.; Gredig, T.; Schuller, I. K. *Europhys. Lett.* **2008**, *83*, 56001.

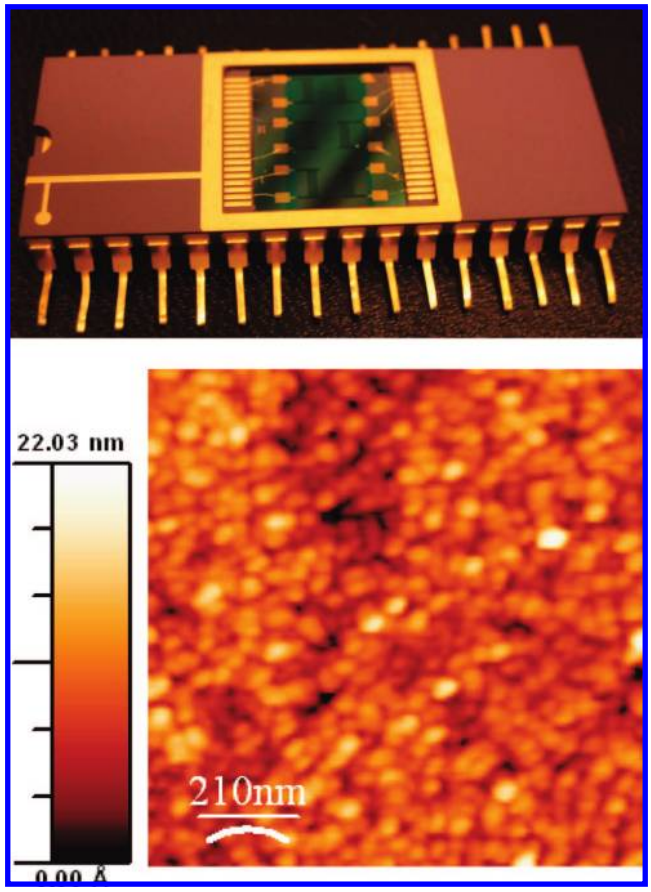

Figure 1. MPc sensor array containing six chemiresistors (50 nm thick Au electrodes, 45 interdigitated pairs of fingers, 5 μm channel spacing, on a 1 μm thick SiO_2 substrate) wirebonded in a dual-inline ceramic package. Also shown is an AFM of a 50 nm thick film of CoPc, with ellipsoidal grains of 50 nm average diameter on the long axis.

During dosing, the chamber temperature was maintained at 50.0 ± 0.1 °C by the use of a Haake F8 constant temperature bath. Zero-grade air was used as the carrier gas for dosing studies, with a constant flow rate of 500 sccm (standard cm^3 per min). Analyte vapors were introduced into the chamber through mass flow controllers (MKS Instruments, Inc. model 1497A, 10 and 1000 sccm) in conjunction with impinger flasks. Analyte concentrations in ppm were calculated from published vapor pressure data[35] using the Clausius−Clapeyron equation; dose concentrations were determined by flask temperature, flow rate through the flask, and dose dilution in the carrier gas. Solenoid valves were placed before and after the impinger flasks to prevent analyte cross-contamination, and a four-way valve was placed before the sensor chamber in order to saturate the gas line with analyte vapor before introduction into the chamber. A Labview VI program was used to control all instruments and record data.

Analytes were chosen to span a range of $-\Delta H^{\circ}_{BF_3}$ and β_2^H basicities. These included dichloromethane, nitromethane, acetonitrile, 2-butanone, di-*n*-butyl ether, trimethyl phosphate, water, isophorone, dimethyl methylphosphonate (DMMP), dimethyl sulfoxide (DMSO), *N*,*N*-dimethylformamide (DMF), and triethylamine (Table 1). All analytes were purchased in analytical purity (99.5+%) from Aldrich with the exception of isophorone (Acros) and DMMP (Strem). Analytes were dried over 4 Å molecular sieves (Fisher) before use. Dichloromethane, nitromethane, acetonitrile, and 2-butanone were dosed at concentrations of 225, 450, 675, and 900 ppm. Di-*n*-butyl ether, trimethyl phosphate, water, isophorone, DMMP, DMSO, DMF, and triethylamine were dosed at 90, 135, 180, and 225 ppm concentrations. The sensor devices were annealed at 70.0 ± 0.1 °C for 1 h before dosing.

Table 1. Lewis Basicities $-\Delta H^{\circ}_{BF_3}$ and Hydrogen Bond Basicities β_2^H for Analytes Studied; Colors Listed Correspond to Color Labeling in All Figures

Analyte	Color Label		$-\Delta H^{o}_{BF_3}$ (kJ mol^{-1})	β_2^H
Dichloromethane	Black	■	10.0	0.05
Nitromethane	Dark Grey	■	37.6	0.25
Acetonitrile	Light Grey	■	60.4	0.31
2-Butanone	Purple	■	76.1	0.48
Di-n-butyl ether	Royal Blue	■	78.6	0.46
Water[a]	Light Blue	■	*82 ± 4*	0.38
Trimethyl Phosphate	Green	■	84.8	0.76
Isophorone	Chartreuse	■	90.6	0.52
DMMP[b]	Yellow	■	*104 ± 13*	0.81
DMSO	Orange	■	105.3	0.78
DMF	Red	■	110.5	0.66
Triethylamine	Wine	■	135.9	0.67

[a] The $-\Delta H^{\circ}_{BF_3}$ value for water was determined from fits of the experimental data for all MPcs in the present study. [b] The $-\Delta H^{\circ}_{BF_3}$ value for DMMP was also determined from experimental fits of all MPcs in the present study; the β_2^H value was estimated from experimental values for dimethyl ethylphosphonate and diethyl methylphosphonate.

Sensor responses were determined from time-dependent current plots at constant voltage. The devices were operated in the space charge limited conduction (SCLC) regime at 8V. Sensor response data for CoPc and H_2Pc were adapted from previously published work by the authors.[25] Sensor responses were calculated as the percent current change during the dose ($\Delta I/I_{baseline} \times 100$) with negative responses for current losses and positive responses for current gains. The responses have been shown to be first order with analyte concentration, so MPc sensitivities to analytes are defined as the slope of the sensor response vs analyte concentration (% ppm^{-1}).[25,36]

2.3. Statistical Methods. All correlation coefficients were determined from linear and nonlinear curve fits in OriginPro 7.5. Recovery time t_{90} data were determined from raw sensor data. Two-way ANOVAs were performed with OriginPro 7.5 using the Tukey method at a significance level of 0.05.[37] Linear discriminant analysis, accuracy estimations, and hierarchical cluster analysis was performed using the *R* statistical computing environment 2.7.1 (LDA function, MASS library; errorest function, ipred library; hclust function, stats package).

(35) Lide, D. R., Frederikse, H. P. R., Eds. *CRC Handbook of Chemistry and Physics*, 74th ed.; CRC Press: Ann Arbor, 1993; Section 9.
(36) Tongpool, R.; Yoriya, S. *Thin Solid Films* **2005**, *109*, 7878–7882.
(37) Armstrong, R. A.; Eperjesi, F.; Gilmartin, B. *Ophthalmic Physiol. Opt.* **2002**, *22*, 248–256.

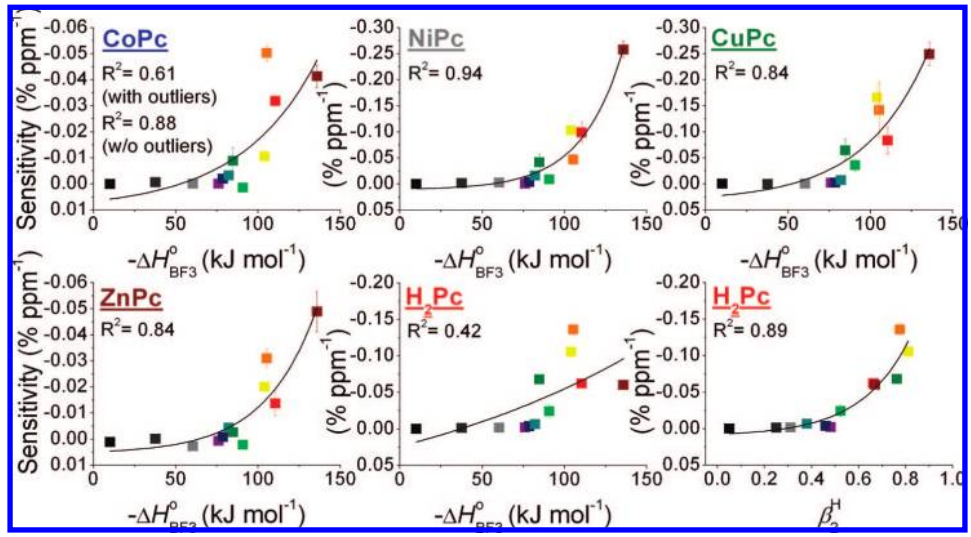

Figure 2. MPc sensitivities plotted versus basicity for all analytes. Exponential fits are shown for all MPcs to Lewis basicity $-\Delta H^{\circ}_{BF_3}$ with the exception of H_2Pc, which is better correlated to hydrogen bond basicity β_2^H. Color coding of analytes is found in Table 1; error bars are present for all points.

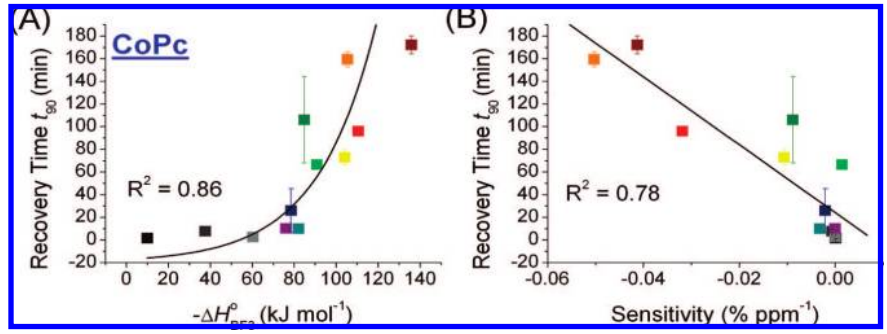

Figure 3. (A) Exponential dependence of CoPc recovery times t'_{90} for 225 ppm doses of each analyte on Lewis basicity $-\Delta H^{\circ}_{BF_3}$. (B) Linear dependence of CoPc recovery times t'_{90} on CoPc sensitivity (% ppm^{-1}). Color coding of analytes is found in Table 1.

3. Results and Discussion

3.1. MPc Sensor Characterization. MPc (M = Co, Ni, Cu, Zn, and H_2) surface morphologies were determined by atomic force microscopy (AFM). The MPcs show differences in granular structure due to variances in crystal lattice; these differences may be caused by metal center or by temperature-induced crystal phase transitions.[16] Granular variability was suppressed in the current study by holding the substrate temperature constant at 25.0 ± 0.1 °C during deposition and closely monitoring the deposition rate (0.2−0.5 Å s^{-1}). All MPc films were found to be textured α phase with ellipsoidal grains of 50 nm average diameter on the long axis (Figure 1).[34] *I*−*V* measurements showed good ohmic behavior at low voltages in all sensors, with space charge limited conductivity (SCLC) occurring in general above 5 V. Operation of MPc IDE sensors in the SCLC regime removes the influence of contact resistance between the MPc film and the electrodes on the relative sensor response; all sensors were operated at 8 V, well within the SCLC regime.[38]

Sensor responses are reported as the percentage change in sensor current at constant voltage on dosing with analytes. Steady-state MPc sensor responses have been found to occur within 30 min of dose exposure.[39−41] Responses and recoveries generally exhibit an initial fast region (∼5 min), accounting for the largest change in sensor current, followed by a slow saturation region. In a previous publication, a model was proposed assigning the fast (kinetic) region of the response and recovery to adsorption of analyte primarily at O_2-free metal centers, and the slow (saturation) response region to competitive displacement of O_2-bound metal centers.[25] It was demonstrated that sensor responses in the 5 min regime for basic physisorption and chemisorption interactions obey first-order kinetics. This behavior dictates that the sensor responses to analytes depend linearly on analyte concentration.[36] In the present study, sensor responses ($\Delta I/I_{baseline} \times 100$) were determined from 5 min doses of analytes at varied concentrations. Selected raw data may be found in Supporting Information, Figure S1. MPc sensitivities (% ppm^{-1}) to individual analytes are thus determined as the slope of the linear fit of the sensor responses versus analyte concentration (Supporting Information, Figure S2A−E).[25]

3.2. Comparison of MPc Sensitivities. Sensitivities (% ppm^{-1}) of all MPcs to all analytes were correlated with the $-\Delta H^{\circ}_{BF_3}$ scale (and the β_2^Hscale in the case of H_2Pc). These data are plotted in Figure 2. There are good exponential fits for sensitivity

(38) Miller, K. A.; Yang, R. D.; Hale, M. J.; Park, J.; Fruhberger, B.; Colesniuc, C. N.; Schuller, I. K.; Kummel, A. C.; Trogler, W. C. *J. Phys. Chem. B* **2006**, *110*, 361–366.

(39) Kolesar, E. S.; Wiseman, T. M. *Anal. Chem.* **1989**, *61*, 2355–2361.

(40) Lee, Y. L.; Tsai, W. C.; Maa, J. R. *Appl. Surf. Sci.* **2001**, *173*, 352–361.

(41) de Haan, A.; Debliquy, M.; Decroly, A. *Sens. Actuators, B* **1999**, *57*, 69–74.

versus Lewis basicity $-\Delta H^{\circ}_{BF_3}$ for CoPc, NiPc, CuPc, and ZnPc. Lewis basicity values ($-\Delta H^{\circ}_{BF_3}$) for DMMP and water are unavailable in the literature, and so they were derived from exponential sensitivity fits of the four MPcs to all analytes. H_2Pc sensing behavior correlates with hydrogen bond basicity, showing a better exponential fit to β_2^H values than to $-\Delta H^{\circ}_{BF_3}$ values. The significance of these exponential dependences will be discussed (*vide infra*).

CoPc sensitivities have been reported previously,[25] with DMSO and isophorone noted as outliers from the general trend of increasing sensitivity with increasing basicity. The unusual sensitivity of CoPc to DMSO ($-\Delta H^{\circ}_{BF_3}$ = 105.34 kJ mol−1) was attributed to hard−soft acid−base properties.[42] The tendency of the soft, electron-rich sulfur of DMSO to bind to the relatively soft cobalt(II) center of CoPc differs from binding of DMSO to the hard Lewis acid BF_3, which would bind to the oxygen of DMSO, leading to the noted disparity in relative binding strength. The binding enthalpy of isophorone (3,5,5-trimethyl-2-cyclohexene-1-one, $-\Delta H^{\circ}_{BF_3}$ = 90.56 kJ mol−1) represents a potential flaw in the $-\Delta H^{\circ}_{BF_3}$ scale. In contrast to cyclohexanone ($-\Delta H^{\circ}_{BF_3}$ = 76.37 kJ mol−1), isophorone is probably overestimated in basicity due to the ability of BF_3 to also bind to the alkene moiety with an enthalpy of 11.8 kJ mol^{-1}.[43]

NiPc, CuPc, and ZnPc follow an exponential dependence on $-\Delta H^{\circ}_{BF_3}$ much more closely than observed in CoPc; they exhibit similarly weak responses to isophorone, but are much less sensitive to DMSO. In general Ni^{2+}, Cu^{2+}, and Zn^{2+} are harder acids than Co^{2+}; they have smaller ionic radii (Co^{2+} = 0.75 Å, Ni^{2+} = 0.69 Å, Cu^{2+} = 0.65 Å, Zn^{2+} = 0.68 Å)[44] and no easily accessible higher oxidation states, while Co^{2+} may be further oxidized to Co^{3+}. Examination of molecular orbital diagrams shows that, on axial binding of electron donors to the metal center, the LUMO of CoPc has d_{z2} character, while the LUMOs of NiPc, CuPc, and ZnPc have d_{π} character.[45] These characteristics make NiPc, CuPc, and ZnPc more likely to form π-bonding interactions with the oxygen in DMSO, while CoPc can form stronger σ-bonding interactions with the sulfur.

3.3. Exponential Dependence of Sensitivity on $-\Delta H^{\circ}_{BF_3}$. It was argued that the analyte sensitivities of CoPc and H_2Pc follow a bilinear dependence on $-\Delta H^{\circ}_{BF_3}$ and β_2^H, respectively.[25] This was attributed to a transition from physisorption to chemisorption at a relative analyte basicity of 73.7 kJ mol^{-1} ($-\Delta H^{\circ}_{BF_3}$) for CoPc and 0.46 units (β_2^H) for H_2Pc. For strong binders ($-\Delta H^{\circ}_{BF_3}$ greater than 73.7 kJ mol−1), chemisorption and coordination at the metal center (CoPc) or the internal protons (H_2Pc) was proposed as the dominant mechanism of sensing. For weak binders ($-\Delta H^{\circ}_{BF_3}$ less than 73.7 kJ mol−1), it is unclear whether chemisorption to the metal center/internal protons or physisorption on the organic ring is the dominant interaction. However, the weak sensor responses observed are consistent with limited charge transfer, whether it arises from weak coordination interactions or physisorption on the organic.

Statistically, the data can be fit equally well by bilinear fits or exponential fits. Exponential fits are consistent with standard models of surface coverage and binding energy. The $-\Delta H^{\circ}_{BF_3}$ scale is a direct measurement of the binding enthalpy of analytes to the Lewis acid BF_3 used as a relative measurement of electron donation/basicity to other Lewis acids.[26] The β_2^H scale is a relative scale that relies indirectly on the binding enthalpy of electron-donating analytes to reference hydrogen-bond acids.[27] The ligand-to-metal binding event (Scheme 1) may be represented by eq 1. The equilibrium constant K for this binding

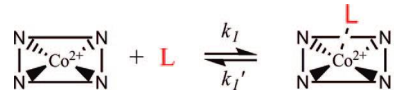

(1)

event should be exponentially related to the enthalpy of binding using the van't Hoff equation[46] and the standard free energy of reaction, eq 2.[47]

$$K = \exp(-\Delta G^{\circ}/RT) \quad (2)$$

$$\Delta G^{\circ} = \Delta H^{\circ} - T\Delta S^{\circ} \quad (3)$$

The entropy change on binding should be approximately equal for all analyte binding interactions; therefore, at constant temperature the equilibrium constant of the reaction is exponentially dependent on the enthalpy of binding (eq 3). An analyte with a high enthalpy of binding would favor the products side of eq 1, leading to a strong sensor response, which exponentially depends on or $-\Delta H^{\circ}_{BF_3}$ or β_2^H

3.4. Exponential Dependence of Sensor Recovery on Basicity. A significant amount of published research is available examining the kinetic behavior of adsorption of molecules onto surfaces with regards to catalysis and oxidation. However, these studies focus predominantly on complex molecular interactions on surfaces of metals and metal oxides.[48] Adsorption rates and coverages on uniform solid surfaces have been described as strongly dependent on apparent Arrhenius parameters, including activation energy E_a.[49] E_a is defined as the minimum amount of energy required to initiate a chemical reaction; this quantity may also be referred to as the Gibbs free energy of activation $\Delta^{\ddagger}$°.[50,51] Application of the Arrhenius equation (eq 4) to the interaction proposed in eq 1 implies that, at constant temperature T, the reaction rate k_1 and the reverse rate k_1' will depend exponentially on $\Delta^{\ddagger}G$° in the absence of transport-limited kinetics.[52]

$$k = A\exp(-\Delta^{\ddagger}G^{\circ}RT) \quad (4)$$

The dependence of the reaction rate k_1 and the reverse rate k_1' on $\Delta^{\ddagger}G$° may be indirectly probed by examining the sensor response and recovery times. Accurate response times are difficult to measure in the kinetic region of the sensor response, and so in the present study recovery times were probed as an indirect measurement of desorption rate. $\Delta^{\ddagger}G$° may be assumed to be the amount of energy required to desorb a molecule from the surface, and should be correlated to the enthalpy of binding; therefore, a large binding enthalpy would imply a slow desorption rate. The recovery time t_{90}' (min) is defined as the time required to recover 90% of the steady-state sensor current.[53]

(42) Gritzner, G. *J. Mol. Liq.* **1997**, *73*, 487–500.
(43) Herrebout, W. A.; van der Veken, B. J. *J. Am. Chem. Soc.* **1997**, *119*, 10446–10454.
(44) Shannon, R. D. *Acta Crystallogr.* **1976**, *A32*, 751–767.
(45) Liao, M. S.; Scheiner, S. *J. Chem. Phys.* **2001**, *114*, 9780–9791.
(46) Garrone, E.; Areán, C. O. *Chem. Soc. Rev.* **2005**, *34*, 846–857.
(47) Espenson, J. H. *Chemical Kinetics and Reaction Mechanisms*; McGraw-Hill, Inc.: New York, 1981.
(48) Kevan, S. D. *J. Mol. Catal. A: Chem.* **1998**, *131*, 19–30.
(49) Zhdanov, V. P. *Surf. Sci. Rep.* **1991**, *12*, 183–242.
(50) Atkins, P. *Physical Chemistry*, 6th ed.; W. H. Freeman and Co.: New York, 2000.
(51) McQuarrie, D. A.; Simon, J. D. *Physical Chemistry: A Molecular Approach*; University Science Books: Sausalito, CA, 1997.
(52) Atkins, P.; Jones, L. *Chemistry: Molecules, Matter, and Change*, 4th ed.; W. H. Freeman and Co.: New York, 2000.
(53) Liu, C. J.; Hsieh, J. C.; Ju, Y. H. *J. Vac. Sci. Technol., A* **1996**, *14* (3), 753–756.

Table 2. Correlation constants for linear fits of two-MPc sensitivity comparisons (Supporting Information, Figure S4A−E)

	CoPc	NiPc	CuPc	ZnPc	H_2Pc
H_2Pc	0.61	0.25	0.59	0.48	1
ZnPc	0.78	0.80	0.90	1	0.48
CuPc	0.63	0.84	1	0.90	0.59
NiPc	0.48	1	0.84	0.80	0.25
CoPc	1	0.48	0.63	0.78	0.61

CoPc t'_{90} values for 225 ppm doses of each analyte are plotted against $-\Delta H^{\circ}_{BF_3}$ in Figure 3A; t'_{90} values are plotted against CoPc sensitivities (% ppm^{-1}) in Figure 3B. It is noted that experimental recovery times can be influenced by low vapor pressure analytes sticking to the walls of the sensor chamber. Analytes with long recovery times tend to also have low vapor pressures, increasing the likelihood of adhesion to the chamber walls; as a result, experimental recovery time should be treated with caution. As shown in Figure 3A, the CoPc t'_{90} values correlate exponentially with the enthalpy of binding; this translates to a linear relationship (Figure 3B) with CoPc sensitivities. The exponential dependence of analyte recovery time t'_{90} on binding enthalpy is evident for all MPcs in this study (Supporting Information, Figure S3A−D). We note that this exponential correlation between binding energy and recovery time does not preclude gas transport from the film to the vapor space affecting the recovery times; it only implies that the transport effects are similar for all analytes studied, which is reasonable since diffusion constants will differ much less than exponential functions of the analyte binding energies. Correlation constants are tabulated (Supporting Information, Table S2) as are recovery times t'_{90} (Supporting Information, Table S3). All MPcs show reasonably good correlation of t'_{90} with the exponential of the binding enthalpy or basicity, and a good linear correlation of t'_{90} to sensitivity, with the exception of H_2Pc.

5. ANOVA of All MPcs. Cross-reactive sensor array applications demand sensors that respond to a broad range of analytes and vary in their relative responses; these sensors are analyzed with pattern-recognition software to identify analytes.[54] MPc sensor data were compared in cross-correlation plots (Supporting Information, Figure S4A−E), and analyzed with a two-way ANOVA (analysis of variance) program. Correlation coefficients for all MPcs are presented in Table 2. CoPc and H_2Pc show the greatest variance from all the other MPcs ($R^2 = 0.25 \leq x \leq 0.78$), while NiPc, CuPc, and ZnPc are all quite similar to one another ($R^2 = 0.80 \leq x \leq 0.90$). This behavior agrees with previously mentioned HOMO−LUMO arguments of binding to electron donors (CoPc bonds through d_σ orbitals, while NiPc, CuPc, and ZnPc bond through d_π orbitals) rather than with classical inorganic binding models such as the Irving−Williams series, which suggests that ZnPc should agree more closely with CoPc behavior.[55]

3.6. Linear Discriminant Analysis. A variety of methods have been explored to selectively identify analytes with cross-reactive sensor arrays, including probabilistic and artificial neural networks (PNN and ANN), linear discriminant analysis (LDA), principal component analysis (PCA), and nearest neighbor (NN) pattern recognition algorithms.[56] Of these, LDA and PCA are among the most popular due to their analysis speed, ease of use, low memory requirements, and statistical accuracy. For example, Anslyn and co-workers have used PCA to selectively identify nitrated explosives such as TNT, RDX, HMX, and tetryl.[21] LDA is generally more useful than PCA because it is a self-consistent method capable of producing greater differentiation and less overlap.[57] In general, LDA and PCA analyses have limited success in separating analytes at varied concentrations due to the superposition of sensor responses, particularly if those analytes have similar interaction mechanisms.[56−61] Incorporation of orthogonal sensing modes, such as the combination of mass spectrometry and surface acoustic wave devices, can help to discriminate between analytes at variable concentrations;[60] without orthogonal sensing, significant overlap between analytes may occur in the LDA plot.[59−61]

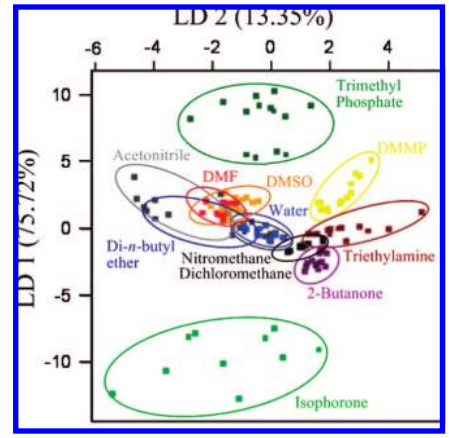

Figure 4. Concentration-independent linear discriminant analysis (LDA) of MPc array sensor responses to all analytes, achieved by normalization to a single ZnPc sensor.

A novel route to remove concentration dependence from the responses of a sensor array to improve the selectivity of LDA has been developed. One well-behaved ZnPc sensor was removed from the LDA, and its concentration-dependent sensor responses were used to normalize all other sensors (Figure 4), thereby removing the concentration dependence of the sensor responses. This normalization technique is effective because of the linear relationship of the MPc sensor responses with analyte concentration. This method was used to identify analytes over a 5× range of concentrations using the MPc sensor array response. The independent variable to be differentiated by LDA was the analyte identity; the dependent variable consisted of a linear combination of all MPc sensor responses. The five different MPc sensor classes result in a five-dimensional LDA, with most analyte separation achieved by the first two dimensions, LD 1 and LD 2 (Figure 4). Reasonable separation was achieved for trimethyl phosphate, isophorone, DMMP, and triethylamine; significant overlap remained for the other analytes.

Weak binders provide most of the problematic overlap within the LDA. These analytes can be easily identified by their recovery times t'_{90}, which are 100−200 times faster than the strong binders (Figure 3A). After independent classification of weak binders by their recovery time, separate LDA analyses

(54) Albert, K. J.; Lewis, N. S.; Schauer, C. L.; Sotzing, G. A.; Stitzel, S. E.; Vaid, T. P.; Walt, D. R. *Chem. Rev.* **2000**, *100*, 2595–2626.
(55) Irving, H.; Williams, R. J. P. *Nature* **1948**, *162*, 746–747.
(56) Shaffer, R. E.; Rose-Pehrsson, S. L.; McGill, R. A. *Anal. Chim. Acta* **1999**, *384*, 305–317.
(57) Greene, N. T.; Morgan, S. L.; Shimizu, K. D. *Chem. Commun.* **2004**, 1172–1173.
(58) Shaffer, R. E.; Rose-Pehrsson, S. L.; McGill, R. A. *Field Anal. Chem. Technol.* **1998**, *2*, 179–192.
(59) Szczurek, A.; Maciejewska, A. *Talanta* **2004**, *64*, 609–617.
(60) Feldhoff, R.; Saby, C. A.; Bernadet, P. *Analyst* **1999**, *124*, 1167–173.
(61) Pardo, M.; Sisk, B. C.; Sberveglieri, G.; Lewis, N. S. *Sens. Actuators, B* **2006**, *115*, 647–655.

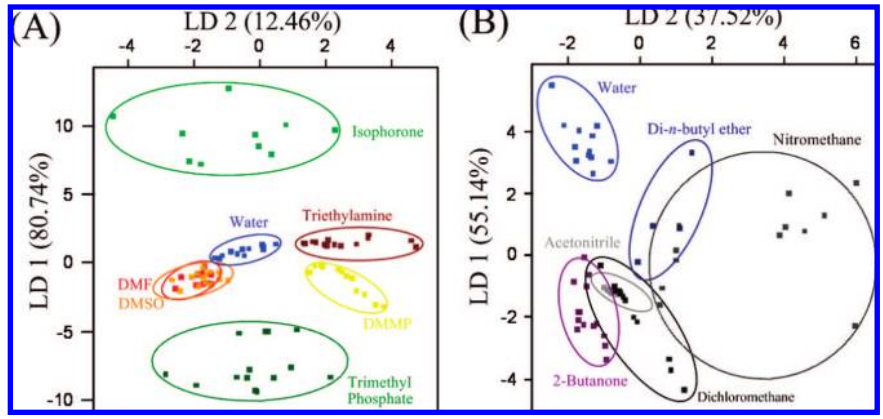

Figure 5. (A) Normalized LDA of MPc array sensor responses to strong binding analytes. (B) Normalized LDA of MPc array sensor responses to weak binding analytes.

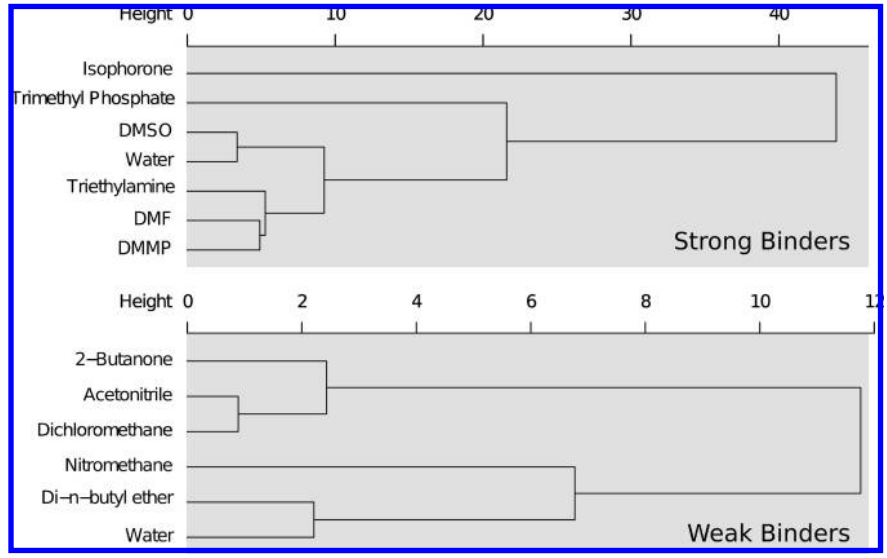

Figure 6. Hierarchical cluster analysis of strong binders and weak binders using complete linkage agglomeration.

Table 3. Accuracy Estimations from 10-Fold Cross-Validation, Bootstrap, and 0.632+ Bias Corrected Bootstrap for Strong Binders, Weak Binders, and All Analytes

	10-fold cross-validation (%)	bootstrap (%)	0.632+ bootstrap (%)
strong binders	96.97	95.11	96.44
weak binders	71.44	70.36	72.45
all analytes	83.32	79.71	82.30

can be performed for the strong and weak binders independently. Classification by recovery time results in an LDA with excellent analyte separation for the strong binders, achieved in the first two LDA dimensions (LD 1 and LD 2); the only overlapping analytes are DMSO and DMF (Figure 5A). This overlap is expected due to the similar basicity values of DMSO and DMF (Table 1). Separation of DMSO and DMF can be achieved with the first and fourth LDA dimensions (LD 1 and LD 4, Supporting Information, Figure S5). LDA of the weak binders alone shows that significant overlap remains (Figure 5B). Accuracy estimations were determined using 10-fold cross-validation, bootstrapping, and 0.632+ bias corrected bootstrap (Table 3).[62] Strong binder and weak binder classification has an estimated accuracy of about 96% and 71%, respectively. If it is unknown which analytes are strong or weak, the estimated accuracy is 80%. Hierarchical cluster analysis using the Euclidian distance metric with complete linkage agglomeration was performed on the strong binders and weak binders (Figure 6). The height differences between the strong binders show a higher degree of separation than that of the weak binders, which is in agreement with the LDA separations. It is noted that initial separation by recovery time is a practical technique since the sensors are operated in pulsed mode (kinetic regime) to reduce the effects of drift on sensor measurement.

4. Conclusion

MPc sensitivities to vapor phase electron donors were found to correlate exponentially with binding enthalpy, consistent with the van't Hoff equation and standard free energy of reaction. MPc sensitivities correlated best with the Lewis base enthalpies $-\Delta H^{\circ}_{BF_3}$, while H_2Pc sensitivities correlated best with the hydrogen bond base enthalpies β_2^H. Sensor recovery times t'_{90}, used as an indirect probe of the analyte desorption rate, were also found to depend exponentially on $-\Delta H^{\circ}_{BF_3}$ (CoPc, NiPc, CuPc, and ZnPc) and β_2^H (H_2Pc). This behavior is in agreement with the Arrhenius equation. The MPc sensitivities showed significant variance among the different analytes. Sensitivities were compared via two-way ANOVA analysis, and it was found

(62) Efron, B.; Tibshirani, R. *J. Am. Stat. Assoc.* **1997**, *92*, 548–560.

that all MPcs vary from one another in a statistically significant way, consistent with electronic structure arguments. Linear discriminant analysis was used to identify analytes. Single sensor normalization of analyte concentration leads to excellent discrimination and identification of analytes, with 95.1% classification accuracy for the strong binding analytes. MPc sensors show promise as robust, inexpensive chemiresistors for incorporation into electronic-nose type applications.[63]

Acknowledgment. We thank AFOSR for funding under MURI Grant F49620-02-1-0288 and NSF CHE-0350571.

(63) Slater, J. M.; Paynter, J.; Watt, E. J. *Analyst* **1993**, *118*, 379–384.

Supporting Information Available: Selected raw sensor data (Figure S1), MPc sensitivity plots for selected analytes (Figure S2A-E), dependence of MPc recovery times t'_{90} on basicity and on MPc sensitivity (Figure S3A-D), MPc cross correlation plots (Figure S4A-E), and full five-dimensional LDA plots for the strong binders (Figure S5). MPc sensitivities for all analytes (Table S1), correlation coefficients for recovery time t'_{90} fits (Table S2), and recovery times t'_{90} for 225 ppm of each analyte for each MPc (Table S3). This material is available free of charge via the Internet at http://pubs.acs.org.

JA803531R